

Neural effective connectivity explains subjective fatigue in stroke

Sasha Ondobaka,^{1,2} William De Doncker,² Nick Ward^{2,3} and Annapoorna Kuppuswamy²

Abstract

Persistent fatigue is a major debilitating symptom in many psychiatric and neurological conditions, including stroke. Post-stroke fatigue has been linked to low corticomotor excitability. Yet, it remains elusive what the neuronal mechanisms are that underlie motor cortex excitability and chronic persistence of fatigue. In this cross-sectional observational study, in two experiments we examined a total of 59 non-depressed stroke survivors with minimal motoric and cognitive impairments using ‘resting state’ magnetic resonance imaging (rs-fMRI), single-pulse and paired-pulse transcranial magnetic stimulation (pp-TMS). In the first session of Experiment 1, we assessed resting motor thresholds (RMTs) - a typical measure of cortical excitability - by applying TMS to the primary motor cortex (M1) and measuring motor-evoked potential in the hand affected by stroke. In the second session, we measured their brain activity with rs-fMRI to assess effective connectivity interactions at rest. In Experiment 2 we examined effective inter-hemispheric connectivity in an independent sample of patients using pp-TMS. We also assessed the levels of non-exercise induced, persistent fatigue using Fatigue Severity Scale (FSS-7), a self-report questionnaire which has been widely applied and validated across different conditions. We employed spectral dynamic causal modelling (sp-DCM) in Experiment 1 and pp-TMS in Experiment 2 to characterise how neuronal effective connectivity relates to self-reported post-stroke fatigue. In a multiple regression we used the balance in inhibitory connectivity between homologue regions in M1 as the main predictor, and have included lesioned hemisphere, RMT and levels of depression as additional predictors. Our novel index of inter-hemispheric inhibition balance was a significant predictor of post-stroke fatigue in Experiment 1 ($\beta = 1.524$, $p = 7.56e^{-05}$, CI[.921, 2.127]) and in Experiment 2 ($\beta = 0.541$, $p = 0.049$, CI[0.002, 1.080]). In experiment 2, depression scores and corticospinal excitability, a measure associated with subjective fatigue, also significantly accounted for variability in fatigue. We suggest that the balance in inter-hemispheric inhibitory effects between primary motor regions can explain subjective post-stroke fatigue. Findings provide novel insights into neural mechanisms that underlie persistent fatigue.

Author affiliations:

1 CoreMind ltd, NW1 8NP, London, UK

2 Department of Clinical and Movement Neuroscience, Institute of Neurology, University College London, WC1N 3BG London, UK

3 NHNN, University College London, WC1N 3BG London, UK

Correspondence to: Sasha Ondobaka

CoreMind ltd

13 Hawley Crescent

NW1 8NP, London

UK

E-mail: sasha@coremind.net

Running title: Effective connectivity explains fatigue

Keywords: post-stroke fatigue, inter-hemispheric inhibition, dynamic causal modelling, paired-pulse TMS

Introduction

Fatigue is a major debilitating symptom in many psychiatric and neurological disorders,¹ including stroke. The reported prevalence of fatigue in stroke survivors is as high as 85%, with post-stroke fatigue having a significant impact on stroke survivors' disability, quality of life and mortality²⁻⁴. Fatigue is commonly understood as being induced by repetition of an activity, such as repeated muscle contractions. Whilst such repetition induced muscle fatigue can be altered after a stroke, post-stroke fatigue refers to self-reported persistent fatigue levels unrelated to repetition induced fatigue.⁵ Such self-reported fatigue can co-occur with other affective symptoms such as depression, sleep disturbances and pain^{6,7} and less so with apathy.^{8,9} Despite such co-occurrences, post-stroke fatigue can occur independently and is regarded as an independent condition, a detailed discussion of which can be found elsewhere¹⁰. Several phenomena originating both in the central and peripheral nervous system have been suggested to play a role in development and persistence of post-stroke fatigue.¹¹⁻¹³ Peripherally, high levels of tissue inflammation early after stroke is linked with a subsequent genesis of post-stroke fatigue.¹⁴⁻¹⁶ Centrally, reduced motor cortex excitability measured with transcranial magnetic stimulation (TMS),¹⁷ reduced inhibition of pre-movement inhibition¹⁸ and poor attention¹⁹ have been associated with persistent post-stroke fatigue. Further support for central nervous system involvement in fatigue comes from studies demonstrating functionally impaired motor areas involved in movement preparation²⁰, abnormal functional connectivity²¹ and altered decision making in Parkinson's fatigue.²² Yet, the neurophysiological mechanisms that underlie persistence of post-stroke fatigue remain elusive.²³

We recently hypothesised that features associated with post-stroke fatigue, such as reduced cortical excitability, reduced self-selected movement speeds and increased limb heaviness, could represent a deficit in sensory attenuation (i.e. inability to withdraw attention from a sensory stream).²⁴ Neural control of attention, which selectively enhances and attenuates different sensory inputs, depends on the largely inhibitory interhemispheric connectivity in the parietal and frontal lobes.²⁵⁻²⁸ Interhemispheric inhibition is typically measured with paired-pulse transcranial magnetic stimulation (pp-TMS) by comparing the amplitude of a motor evoked potential (MEP) elicited by stimulation of the primary motor cortex (M1) with or without preceded subthreshold stimulation of the contralateral M1. To better understand mechanisms that underlie post-stroke fatigue (PSF), here we test whether variability in self-

reported PSF is associated with inter-hemispheric effective connectivity. In two separate experiments we employed computational modelling of resting-state functional MRI (rs-fMRI) and paired-pulse pp-TMS to characterise how inter-hemispheric effective connectivity relates to PSF.

Experiments using pp-TMS protocols^{29,30} provide causal evidence that transcallosal connectivity underpins control of attention and cortico-spinal excitability.^{27,29–34} Inter-hemispheric inhibitory effects in the normal functioning brain are not balanced between hemispheres, but exhibit an asymmetry characterised by a net left hemispheric inhibitory dominance in motor cortices^{35–37} and outside primary motor areas (e.g.^{27,34}). Interhemispheric inhibitory balance (IIB) can be quantified using pp-TMS³⁵ or effective connectivity measures derived from neuroimaging (see Friston *et al.*³⁸), by subtracting the inhibitory effects of the two hemispheres from each other ($[L \text{ to } R] - [R \text{ to } L]$). Inter-hemispheric inhibitory effects are mediated by predominantly GABA-ergic neurons that connect homologue regions in the two hemispheres.³⁹ Spectral dynamic causal modelling sp-DCM provides a model-based approach to assess correlations between BOLD signal intensities in different regions.^{38,40} Compared to the classic functional connectivity methods^{41,42}, both sp-DCM and pp-TMS offer complementary methods that can discern the directionality and the valence (net inhibition vs excitation) of the underlying neural effects.

Disturbed IIB balance is observed in various neurological and psychiatric disorders.^{43–51} For example, clinical depression is characterised by a shift in inhibitory dominance away from the left and towards right hemisphere dominance⁴⁸, and excitatory repetitive TMS protocols to left frontal cortex are used to reverse the dominance to significantly decrease depression severity.⁵² In the current study, we reasoned that the nature of inter-hemispheric inhibitory effects could provide a mechanistic explanation for inter-individual variability in severity of PSF. To exclude that depression would compromise statistical inference, we included only non-depressed stroke survivors and, in our analyses, we accounted for variability in depression symptoms. Our main aim was to examine the relationship between inter-hemispheric inhibitory balance of homologue neural populations and subjectively reported PSF severity. Given IIB was previously linked with attentional and affective disorders, we hypothesised that the deviation from the naturally occurring left-hemisphere inhibitory dominance would be positively associated with the severity of persistent self-reported PSF. To test this hypothesis in non-depressed stroke survivors with minimal cognitive and motor impairment, in two

separate experiments we employed sp-DCM of spontaneous resting state fMRI signals and pp-TMS.

Materials and methods

Participants

This is a cross-sectional observational study approved by the Riverside Research Ethics Committee (12/LO/1474) and the London Bromley Research Ethics Committee (16/LO/0714). All stroke survivors provided written informed consent in accordance with the Declaration of Helsinki.

Inclusion criteria

The diagnostic inclusion criteria for recruitment included a clinical diagnosis of a first-time ischaemic or haemorrhagic lesion, date of stroke at least three months from the day of testing and age ≥ 18 years.

Exclusion criteria

To avoid potential sources of bias, the following exclusion criteria were adopted: use of centrally acting medication, no contraindications to TMS and fMRI procedures, depression scores ≥ 11 assessed using the Hospital Anxiety and Depression Scale (HADS) and poor function. Functional screening included upper limb functional tests and cognitive tests. Poor upper limb function was defined as having $<60\%$ of the unaffected limb score in more than one of the following measures: (i) Nine Hole Peg Test (9HPT) to measure finger dexterity; (ii) Action Research Arm Test (ARAT); (iii) Grip strength

Recruitment

Experiment 1 recruitment: rs-fMRI + TMS

Stroke survivors were recruited from the Thames Stroke Research Network from the University College NHS Trust Hospital, Epsom NHS Trust Hospital, Royal Surrey NHS Trust Hospital and from community stroke groups between February 2013 and September 2014. A total of 225 stroke survivors were screened on the above-mentioned eligibility criteria. Eligibility criteria were met by 78 participants, of which we have recruited 70 for the TMS session (reported in Kuppuswamy *et al.*¹⁷). 18 of the 70 stroke survivors additionally took part in the

resting state fMRI scanning session and were included in this study and their data was used for the reported analyses. There was one participant with a missing date of birth. The sample consisted of eighteen (two female) non-depressed, ischemic or haemorrhagic stroke survivors with a mean age of 58.68 ± 10.30 (mean \pm SD), tested 4.03 ± 3.97 (mean \pm SD) years post stroke.

Experiment 2 recruitment: paired-pulse TMS (pp-TMS)

Stroke survivors were recruited via the Clinical Research Network from the University College NHS Trust Hospital, departmental Stroke Database and the community between October 2017 and June 2019. A total of 132 stroke survivors were screened on the above-mentioned eligibility criteria. Eligibility criteria were met by 113 stroke survivors, of which 41 were recruited for the pp-TMS experiment. The pp-TMS sample consisted of 41 (nine females) non-depressed, ischemic or haemorrhagic stroke survivors with a mean age of 62.37 ± 12.63 (mean \pm SD), tested 5.46 ± 5.76 (mean \pm SD) years post stroke.

Fatigue and depression measurements

In both experiments, we measured fatigue using the Fatigue Severity Scale (FSS-7), a widely used and validated self-report questionnaire. FSS responses range from 1-7 with an average score of seven being the highest fatigue and a score of one reflecting no fatigue whatsoever.⁹ We measured depression with the Hospital Anxiety and Depression Scale (HADS) that is typically used in a clinical setting to assess anxiety and depression in patients with physical symptoms. With a maximum score of 21, normal scores range from 1-7, 8-10 being borderline cases, and 11 and above abnormal or depressed cases.

Experiment 1 methods: rs-fMRI and TMS

In two experimental sessions, we measured low-frequency spontaneous fluctuations in the rs-fMRI signal and resting motor thresholds (RMTs), a typical measure of corticospinal excitability. Our use of RMTs was motivated by its association with fatigue in our previous work. For full details of the TMS procedure used in the first session please refer to our previous work.¹⁷ In the second session, participants underwent an eyes-open twelve-minute rs-fMRI using a standard scanning protocol. Scanning was performed at the Wellcome Centre for Human Neuroimaging using a 3T Trio scanner (Erlangen, Siemens). All participants underwent a single scanning session during which a T2*-weighted MRI transverse echo-planar

images (EPI) were acquired using a 12-channel head coil. The resting block comprised 200 volumes of 32 slices, with a 30ms echo time (TE) and a repetition time (TR) of 2.175 s (4.5 x 4.5 x 4.5 mm voxels). Participants were instructed to lie within the scanner, to keep their eyes closed, to remain awake and to restrict their movement as much as possible until further instructed. A high resolution T1-weighted anatomical images (1.3 x 1.3 x 1.3 mm voxels; 176 partitions, FoV = 256 x 240, TE = 2.48ms, TR = 7.92ms, FA = 16°) and a field map (TE1 = 10ms and TE2 = 12.46ms, 3x3x3mm resolution, 1mm gap) were also acquired. This was used to create B0 fieldmaps used by the SPM Fieldmap Toolbox to unwarp the functional images.

fMRI pre-processing

We performed conventional functional imaging pre-processing using SPM12 (www.fil.ion.ucl.ac.uk/spm), including the removal of the first four volumes, realignment, spatial normalization with 3mm cubic voxels, a spatial smoothing of 6 mm FWHM and nuisance variable regression. The nuisance regressors included 18 motion parameters (six head motion parameters and their first and second derivatives) and the average signal strength extracted from 6mm spheres from two (cerebrospinal fluid and white matter) reference regions with the following MNI (x, y, z) coordinates: 19 -34 18 and 27 -18 32. This set of nuisance variables incidentally removes low-frequency fluctuations normally associated with global confounds.

Dynamic causal modelling of effective connectivity

Sp-DCM provides a model-based approach to understand correlations between BOLD signal in different brain regions. Compared to the classic functional connectivity methods that mainly describe correlations between signal intensities in different regions,^{41,42} sp-DCM offers a possibility to discern the directionality and the valence (net inhibition vs excitation) of the underlying neural influences.^{38,40} Sp-DCM models extrinsic (i.e. between regions) and intrinsic (i.e. within region) effective connectivity in the selected brain regions of interest based on the estimated cross-spectra (cross-covariances in the frequency domain) of the extracted BOLD time-series. An advantage of using a model-based approach like DCM is the opportunity to infer the biologically plausible inter-hemispheric neural interactions that underlie fatigue, as compared to investigating the dynamics in the measured EEG or fMRI signals. Examination of the model parameter values that provide best fit for the observed fMRI signals allow characterisation of the biologically plausible inter-hemispheric connectivity patterns that best explain reported fatigue.

To employ sp-DCM we extracted rs-fMRI BOLD time-series from bilateral primary motor cortices (M1; 30 -24 64; -30 -20 66), anterior insular cortices (38 16 2; -36 16 0), thalamus (12 -12 10; -12 -12 10) and caudate nuclei heads (14 12 14; -14 12 14). Additionally, we included the three cortical midline regions of interest (ROIs): the supplementary motor area (SMA; 0 -6 58) and the two key default mode regions, ventromedial prefrontal cortex (vmPFC; 0 50 -4) and posterior cingulate cortex (PCC; 0 -52, 24). Inclusion of midline regions was a pragmatic choice that was expected to result in a model that better captures global endogenous neural fluctuations. Exact locations of the centres of the 8mm ROI spheres, indicated above in MNI coordinates, were determined by using NeuroSynth meta-analysis maps. NeuroSynth (<http://neurosynth.org>) is an online platform for large-scale automated meta-analysis of published neuroimaging results that provides posterior probabilities of a specific term being used in the abstract of the analysed publications (e.g. primary motor cortex) conditional on the presence of activation in a chosen voxel. We selected the voxels with the highest posterior probability of being associated with the terms of the 11 chosen ROIs included to capture the global neural fluctuations of both hemispheres (**Fig. 1**). Visual inspection of structural images showed no apparent lesions in any of the selected ROIs. The resulting specified model consisted of a fully connected architecture with 110 extrinsic connections and 11 intrinsic connections (**Fig. 1**).

Participants-specific Bayesian estimation of effective connectivity parameters

At the participants-specific level of analysis, we estimated the strength of all effective connectivity parameters for each participant using a standard Bayesian inversion scheme (Variational Laplace⁵³). We used a parametric empirical (PEB, using `spm_dcm_peg_fit` in SPM 12) model that furnishes a more efficient and robust estimation of effective connectivity parameters by using a group mean as empirical prior.⁵⁴ During the iterative model estimation (i.e., Bayesian model inversion) procedure, the connectivity parameter strengths representing biologically plausible extrinsic and intrinsic effects are optimised to generate cross spectral density (CSD) so as to fit this CSD to the measured CSD (which is generated from the measured BOLD data). DCM uses negative variational free energy to approximate the log-evidence that a particular model of connectivity patterns fits or explains the observed fluctuations in the region-specific BOLD time-series. In DCM, estimated positive values of extrinsic parameters represent excitatory effect and negative values index inhibitory effect from region A to region

B, while their absolute values represent percent estimated activity change of this effect (effect size). The participants' specific estimates were used to compute an index of inter-hemispheric connectivity used in subsequent group-level analysis (see **Table 1** for M1 summary).

Using participants-specific posterior expectations for each effective connection, we computed the inter-hemispheric inhibitory balance (IIB) index for primary motor cortex, the anterior insular cortex, caudate and the thalamus by subtracting right-to-left hemisphere parameter values from left-to-right parameter values [IIB = (L to R) - (R to L)]. IIB index characterises the nature of normally occurring inter-hemispheric inhibitory balance in the individual 'resting' brain. Negative IIB values reflect stronger left to right net inhibitory effect, whereas positive values reflect stronger inhibitory right to left effect.

Group-level multiple regression of FSS values from the inhibitory balance (IIB) indices

Finally, at the between-participants (group) level analysis, to explain individual differences in subjectively reported FSS (fatigue) scores we used the participants-specific IIB indices and the interaction between lesioned hemisphere (left vs right) and IIB indices. The interaction term was included to test for a potential confounding effect of the lesioned hemisphere. We used classic multiple linear regression analysis in R software (RStudio Version 1.2.5033) to test whether the explanatory variables significantly explain variance in the FSS target variable. We applied Bonferroni correction to a chosen significance threshold of $p < 0.05$ to control for false positives over four tests of inter-hemispheric inhibitory balance (IIB) in M1, insula, caudate and the thalamus. We used Hotteling's t -test to examine whether there were statistical differences in explanatory power of the four IIB indices, i.e., to test for the interaction in the strength of associations. In a second multiple regression model, we tested whether IIB uniquely explains FSS when HADS depression scores and individual resting motor thresholds (RMTs) are added as independent explanatory variables. In a third and final model, we also included age and sex as independent explanatory variables to control for their influence. Best fitting model was determined using the Bayesian Information Criterion (BIC), with a lower BIC indicating a better fitting model. Assumptions of normality and homoscedasticity of the residuals for each linear regression model were assessed visually using quantile-quantile normal plots and fitted- versus residual-value plots.

Experiment 2 methods: Paired-pulse TMS (pp-TMS)

In experiment 2, we used pp-TMS to quantify the extent of interhemispheric inhibition between the homologue primary motor cortices. Experiment 2 was motivated by the findings from Experiment 1 and has aimed to provide an inter-methodological cross-validation using pp-TMS. A conditioning TMS pulse (CP) was applied to the M1 on one hemisphere, followed 10 milliseconds later by a test TMS pulse (TP) delivered to the M1 of the other hemisphere. Trials using double pulses (CP-TP) were randomly intermixed with those containing TP alone, with 20 trials for each condition, giving a total of 40 trials. The inter-trial interval was set to 7 seconds (± 1.4 seconds). IHI was calculated as the amplitude of the conditioned MEP in the double-pulse trials (CP-TP) relative to the amplitude of the test MEP when TP was delivered alone: $TP - (CP-TP)$. This process was then repeated for the other hemisphere, giving us a measure of IHI from left to right hemisphere (IHI_{LtoR}: CP applied to left hemisphere and TP applied to right hemisphere) and from right to left hemisphere (IHI_{RtoL}: CP applied to right hemisphere and TP applied to left hemisphere).

Surface Electromyogram and Transcranial Magnetic Stimulation

Electromyogram (EMG) recording were carried out on the first dorsal interosseous (FDI) muscle of both hands using neonatal prewired disposable electrodes (1041PTS Neonatal Electrode, Kendell) in a belly-tendon montage. The ground electrode was positioned over the flexor retinaculum of the hand. The signal was band pass filtered (20-1000 Hz), amplified with a gain of 1000 (D360, Digitimer, Welwyn Garden City, UK), digitized at 5 kHz (Power1401, CED, Cambridge, UK) and recorded with signal version 6.04 software (CED, Cambridge, UK). TMS was delivered using two magnetic stimulators (Magstim 200², Magstim, Whitland, Wales), each connected to a figure-of-eight coil (70mm diameter for the TP and 50mm diameter for the CP). The magnetic coil for the TP was held tangentially on the scalp at an angle of 45° to the mid-sagittal plane to induce a posterior-anterior (PA) current across the central sulcus. The magnetic coil for the CP was held at an angle of 90° to the mid-sagittal plane. The subjects were instructed to stay relaxed with their eyes open and their legs uncrossed. The motor 'hotspot' of the FDI muscle for each hemisphere was determined as previously.¹⁷ Both coils were held at the hotspot of the FDI muscle in each hemisphere during the stimulation protocol. The stimulator setting for both stimulators was adjusted to produce a target MEP size of 0.5mV. This was defined as the stimulator setting (determined to the nearest 1% of MSO) required to evoke a peak-to-peak MEP amplitude of $\geq 0.5\text{mV}$ in a minimum of 5 of 10 consecutive trials.

TMS Data Analysis

The data files were extracted from Signal into Matlab and were analysed offline using custom-written routines in Matlab (2018a, MathWorks). MEP peak-to-peak amplitude was measured on a trial-by-trial basis from the acquired EMG signal without applying any additional filters. Resting EMG was defined as the root mean square (rms) across all trials for each participant in the 100ms preceding the TMS pulse of each trial. Thresholds set at four times these levels were used to identify any muscle contraction preceding the stimulation. All trials were then visually inspected to ensure that no build-up of EMG was apparent before the TMS. Trials containing outlier MEP amplitudes (Grubb's test, $p < 0.005$) were also excluded from the final analysis. On average 7.9% of TMS trials were excluded across all stroke survivors with a minimum of 15 trials per condition.

Identical to the procedure in Experiment 1, the interhemispheric inhibitory balance (IIB) index was computed by subtracting the right-to-left IHI from the left-to-right IHI ($IIB = IHI_{LtoR} - IHI_{RtoL}$). IIB index characterizes the naturally occurring interhemispheric inhibitory balance in the individual 'resting' brain. Negative IIB values reflect stronger left-to-right inhibition, whereas positive values reflect stronger right-to-left inhibition.

Group-level multiple regression of FSS values from the inhibitory balance (IIB) indices

To explain individual differences in subjectively reported FSS-7 (fatigue) scores, we have again implemented a multiple linear regression in R (RStudio Version 1.2.5033). We used the same full model as in Experiment 1 including IIB and the interaction between lesioned hemisphere and IIB, HADS depression scores and resting motor thresholds (RMTs). Assumptions of normality and homoscedasticity of the residuals were assessed visually using quantile-quantile normal plots and fitted- versus residual-value plots.

Data availability

Raw data can be made available upon request.

Results

Participants' characteristics

In experiment 1, six stroke survivors had a right hemisphere stroke and eleven had a left hemisphere stroke, see **Table 2**. Participant characteristics indicated low cognitive impairment,

indexed by unaffected mental speed (SDMT scores of 1.25 ± 0.42). Participants also showed low motoric impairment, reflected in the measured 9HPT (77.73 ± 33.06 %), ARAT scores (96.01 ± 11.17 %) and preserved grip strength (88.67 ± 22.14 %) of the unaffected side. In experiment 1, ischaemic strokes were predominantly lacunar (localised and small in size), whereas the three haemorrhagic strokes were associated with an extensive cortical damage. We ensured that none of the 11 ROIs used to build our DCM model had any noticeable structural damage.

In experiment 2, twenty stroke survivors had a left hemisphere stroke and twenty-one had a right hemisphere stroke. Participant characteristics indicated low cognitive impairment, indexed by unaffected mental speed (SDMT scores of 1.18 ± 0.46). Participants also showed low motoric impairment, reflected in the measured 9HPT (89.31 ± 22.38 %), ARAT scores (99.60 ± 1.56 %) and preserved grip strength (95.55 ± 15.45 %) of the unaffected side. MRI data was not consistently available for the participants in Experiment 2. Participants in the two experiments did not differ in any of the relevant indices, see **Table 3**.

Inter-hemispheric balance explains level of persistent fatigue

The result from the multiple linear regression analysis from Experiment 1 showed that the individual IIB in the motor cortex inferred from sp-DCM explains reported levels of persistent fatigue. IIB in M1 explained reported FSS scores ($\beta = 1.524$, $p = 7.56e^{-05}$, CI[.921, 2.127]; **Fig. 2**), whereas lesioned hemisphere did not influence the IIB-FSS association ($\beta = .056$, $p = .912$, CI[-1.013, 1.125] for IIB x lesioned hemisphere interaction), accounting for 63% of the variability in the reported fatigue scores (adjusted $R^2 = .629$). We did not observe any significant effects at the Bonferroni corrected threshold of .0125 when the FSS values were regressed on the IIB scores from the insula ($\beta = -0.4850$, $p = 0.327$, CI[-1.505, 0.535]), caudate ($\beta = 0.4385$, $p = 0.3288$, CI[-0.487, 1.364] and the thalamus ($\beta = -0.9613$, $p = 0.0415$, CI[-1.881, -0.042]). Moreover, Hotelling t -tests revealed that FSS-M1 IIB correlation was significantly different from the correlations between FSS and insula IIB ($t = 4.550$, $p < .001$), caudate IIB ($t = 3.440$, $p = .004$) and thalamus IIB ($t = 7.364$, $p < .001$).

Additional multiple regression analysis included individual RMTs and HADS_{Depression} scores next to IIB scores to test and account for effects of cortical excitability and depression in a single model. The results demonstrated IIB was a unique significant explanatory variable ($\beta =$

1.524, $p = .026$, CI[.163, 2.120], BIC = 67.37) of variability in FSS fatigue scores. While the interaction between lesioned hemisphere and IIB was not a significant predictor of FSS-7 ($\beta = -.051$, $p = 0.924$, CI[-1.177, 1.075]), nor were HADS_{Depression} and RMT ($\beta = 0.357$, $p = 0.256$, CI[-.291, 1.005] and $\beta = 0.422$, $p = 0.352$, CI[-.521, 1.364] respectively). The multiple regression model that included participant's age and sex as additional predictors did not significantly improve the model fit (BIC = 72.76). However, when accounting for the effect of age and sex, IIB was still a unique significant explanatory variable ($\beta = 1.179$, $p = .037$, CI[.088, 2.270]) of variability in FSS fatigue scores while none of the other additional explanatory variables were significant predictors of FSS-7.

In an independent sample of stroke survivors, in Experiment 2 we used individual IIB in the motor cortices, directly measured with pp-TMS, to explain reported levels of persistent fatigue. Again, we used multiple regression analysis using the same explanatory variables as in the best fitting model in Experiment 1: lesioned hemisphere, RMTs and HADS depression scores. In line with findings from Experiment 1, results showed evidence that IIB in M1 explains individual FSS scores ($\beta = 0.541$, $p = 0.049$, CI[0.002, 1.080]), while lesioned hemisphere interaction with IIB was not a significant predictor ($\beta = -0.122$, $p = 0.874$, CI[-1.682, 1.437]). Next to IIB, HADS depression score ($\beta = 0.981$, $p = 0.001$, CI[0.419, 1.543] and RMT ($\beta = 0.542$, $p = 0.043$, CI[0.018, 1.066]) were also independent significant predictors of FSS. Stroke survivors with low persistent post-stroke fatigue had low corticospinal excitability and low self-reported depression scores; survivors with high fatigue had relatively high corticospinal excitability and high depression scores.

Discussion

Optimal inter-hemispheric inhibition balance (IIB) is fundamental for healthy neurological and psychological functions. Our results show an association between individuals' levels of IIB in primary motor cortices (M1) and their reported levels of persistent post-stroke fatigue. These findings were replicated in two independent experiments using complementary neuroscientific methodology - computational modelling of resting state fMRI signals and paired-pulse TMS measuring inter-hemispheric inhibition. Below we discuss our findings in light of prior work and theorise about the functional and biological mechanisms that underlie inter-hemispheric balance.

Inter-hemispheric inhibitory balance (IIB) and post-stroke fatigue

Healthy brains exhibit a left-dominant IIB. We showed enhanced right hemisphere interhemispheric inhibitory dominance is related to the experience of high post-stroke fatigue. Higher left hemisphere inter-hemispheric inhibitory dominance was associated with low post-stroke fatigue, with inter-hemispheric inhibitory balance explaining a large proportion of inter-subject variability in measured fatigue severity. Our results are in keeping with findings that link chronic fatigue in multiple sclerosis to inter-hemispheric balance disturbances indexed by the measured EEG activity.²¹ This indicates that similar biological mechanisms might be at the base of persistent fatigue state, irrespective whether it was initially triggered by a stroke or multiple sclerosis.²⁴ Generally, the opposite pattern of inter-hemispheric connectivity in post-stroke fatigue is in agreement with the disturbed patterns of inter-hemispheric connectivity associated with many neurological and psychiatric disorders.^{43,44,46-51}

Particularly relevant is the agreement with the typically observed right hemisphere inhibitory dominance and the elevated corticospinal excitability in clinical depression⁴⁸, a multifaceted disease that includes fatigue as a principal symptom. Our results from the pp-TMS experiment that reveal an association between self-reported depression and fatigue are in congruence with the view in which depression and persistent fatigue partly share a common underlying mechanism. Notably, overall, the studied population had an average HADS depression score of 4.3 (exp. 1) and 4.6 (exp. 2) out of 21 (8 being borderline and 11 abnormal threshold), making depression an unlikely confound. Subjective fatigue measured by FSS-7 is shown to be unrelated to apathy, a syndrome that could be confused with fatigue. Original FSS-9 scale included an item assessing motivation that is now excluded due to its repeated inconsistency with fatigue, rendering the confusion unlikely (see⁹). The affected hemisphere did not influence our findings as indicated by the absence of its significant interaction with IIB.

Post stroke fatigue and cortical excitability

Previously we showed an association between self-reported fatigue and cortico-spinal excitability in a sample of 70 patients with PSF.¹⁷ Current finding of a negative association between corticospinal excitability and PSF from Experiment 2 is well in line with the main findings from our previous work. Whereas cortical excitability and IIB were both independent explanations for fatigue in Experiment 2, IIB was a sole significant predictor of fatigue in Experiment 1, over and above the contributions of cortical excitability that showed similar non-significant pattern. Distinct results associating both IIB and cortical excitability to PSF beg the

question how we can synthesise the effects of these two physiological measures on fatigue. One simple hypothesis that could provide a synthesis of these results is that resting cortical excitability causally depends on inter-hemispheric connectivity. This view is congruous with data from repetitive transcranial stimulation (rTMS) work showing that inhibitory stimulation to M1 effects cortical excitability in the contralateral M1.^{32,33} Similarly, changes in cortical excitability in one M1 elicited by stimulating homologue area in the other hemisphere are dependent on transcallosal connectivity.⁴⁴ Dependency of cortical excitability on intra- and inter-hemispheric cortical connectivity emphasises crucial importance to increase understanding how wider network effect local excitation-inhibition dynamics. Although, M1-IIB effect differed significantly from the other examined IIB effects, we do not provide evidence that M1-IIB is an exclusive explanation for PSF. Enhanced knowledge of causal network interactions using effective connectivity methods could improve future treatments aiming to modulate IIB to ameliorate PSF and related affective disorders.

Functional and neural mechanisms of inter-hemispheric inhibitory balance

A fundamental question is what are the functional and biological mechanisms that underlie inhibitory inter-hemispheric balance? One proposal links variation in intra- and inter-hemispheric effects to asymmetry in the autonomic nervous system activity.⁵⁵ Craig proposes that left hemisphere shows stronger association with processing of parasympathetic information and right hemisphere with processing of sympathetic information. Perhaps, the inhibitory dominance of left hemisphere over right hemisphere as shown by TMS inter-hemispheric protocols reflects, or is even driven by, the balance of autonomic functions of the two hemispheres. The shift in balance to right hemisphere dominance (sympathetic dominance) could also explain the inability to attend away from current sensory inputs (poor sensory attenuation). Recent work proposed poor sensory attenuation of incoming sensory information as a potential mechanism underpinning post stroke fatigue.²⁴ Further research is necessary to understand the role of autonomic activity in inter-hemispheric effects and consequently its effect on post-stroke fatigue and other affective disorders.

Limitations

The exclusion of stroke survivors with high levels of depression, motoric and cognitive impairments could limit generalisability of our findings. In this study, stroke survivors with high levels of depression were excluded to isolate the group with fatigue without psychiatric

comorbidities, as clinical depression has already been associated with aberrant inter-hemispheric connectivity.^{48,52} The exclusion of stroke survivors with depression has not introduced any potential bias to the interpretations of the data as the focus of the study was to understand biological mechanisms of post-stroke fatigue. To account for the relationship between depression and fatigue, measures of depressive symptoms were included in the analysis. The study did not include explicit measures of apathy, a motivational syndrome that shares attributes with persistent fatigue. However, fatigue, as measured by FSS-7, has been shown to be extraneous to motivation and apathy making it unlikely to compromise content validity of our fatigue measure⁹. We have also excluded participants with large motoric and cognitive impairments, a pragmatic choice that should not lead to limited generalisability of our findings to fatigued stroke survivors with larger impairments.

Future directions

The strong explanatory power of resting inter-hemispheric inhibitory connectivity makes it a potential target for new PSF intervention protocols using transcranial magnetic or electric stimulation. More specifically, brain stimulation methods aiming to recover physiological inter-hemispheric inhibition balance and optimal cortical excitability could be utilised to ameliorate fatigue symptoms (e.g.⁵²). An advantage of using a model-based approach like dynamic causal modelling is the opportunity to infer the biologically plausible inter-hemispheric neural connectivity that underlies fatigue, as compared to investigating the dynamics in the measured EEG or fMRI signals. Examination of the model parameter values that provide best fit for the observed fMRI signals allow characterisation of the biologically plausible directionality and the sign of the inter-hemispheric connectivity patterns that best explain reported fatigue. A promising avenue for the future is to combine patient specific characterisation of interhemispheric balance, inferred from TMS, fMRI or EEG signals, with neuro-stimulation protocols that apply TMS, DC or AC current to rebalance the disturbed inter-hemispheric dynamics. A first step on this avenue would be to better understand the autonomic and central nervous system mechanisms behind the reversal of inter-hemispheric dominance.

Conclusion

We suggest that the balance in inter-hemispheric inhibitory connectivity between primary motor regions is involved in persistence of subjective fatigue. Our findings that post-stroke fatigue is associated with altered effective connectivity in M1 support the importance of optimal inter-hemispheric inhibitory balance for healthy brain functioning.

Acknowledgements

We would like to acknowledge the help of Ms Cora Burke and Ms Isobel Turner who were involved in data collection of fMRI data.

Funding

This work was supported by the Wellcome Trust (202346/Z/16/Z) and Stroke Association (SA2015/02).

Competing interests

The authors report no competing interests.

References

1. Chaudhuri A, Behan PO. Fatigue in neurological disorders. *The lancet*. 2004;363(9413):978-988.
2. Glader E-L, Stegmayr B, Asplund K. Poststroke fatigue: a 2-year follow-up study of stroke patients in Sweden. *Stroke*. 2002;33(5):1327-1333.
3. van de Port IGL, Kwakkel G, Schepers VPM, Heinemans CTI, Lindeman E. Is fatigue an independent factor associated with activities of daily living, instrumental activities of daily living and health-related quality of life in chronic stroke? *Cerebrovasc Dis Basel Switz*. 2007;23(1):40-45.
4. Naess H, Nyland H. Poststroke fatigue and depression are related to mortality in young adults: a cohort study. *BMJ Open*. 2013;3(3).
5. Kluger BM, Krupp LB, Enoka RM. Fatigue and fatigability in neurologic illnesses: proposal for a unified taxonomy. *Neurology*. 2013;80(4):409-416.
6. Wu S, Barugh A, Macleod M, Mead G. Psychological associations of poststroke fatigue: a systematic review and meta-analysis. *Stroke J Cereb Circ*. 2014;45(6):1778-1783.
7. Cumming TB, Packer M, Kramer SF, English C. The prevalence of fatigue after stroke: A systematic review and meta-analysis. *Int J Stroke Off J Int Stroke Soc*. 2016;11(9):968-977.
8. Douven E, Köhler S, Schievink SH, et al. Temporal associations between fatigue, depression, and apathy after stroke: results of the cognition and affect after stroke, a prospective evaluation of risks study. *Cerebrovasc Dis*. 2017;44(5-6):330-337.
9. Johansson S, Kottorp A, Lee KA, Gay CL, Lerdal A. Can the Fatigue Severity Scale 7-item version be used across different patient populations as a generic fatigue measure--a comparative study using a Rasch model approach. *Health Qual Life Outcomes*. 2014;12:24.
10. De Doncker W, Dantzer R, Ormstad H, Kuppuswamy A. Mechanisms of poststroke fatigue. *J Neurol Neurosurg Psychiatry*. 2018;89(3):287-293.
11. Staub F, Bogousslavsky J. Fatigue after stroke: a major but neglected issue. *Cerebrovasc Dis Basel Switz*. 2001;12(2):75-81.
12. De Groot MH, Phillips SJ, Eskes GA. Fatigue associated with stroke and other neurologic conditions: Implications for stroke rehabilitation. *Arch Phys Med Rehabil*. 2003;84(11):1714-1720.
13. Kutlubaev MA, Mead GE. One step closer to understanding poststroke fatigue. *Neurology*. 2012;79(14):1414-1415.
14. Ormstad H, Aass HCD, Amthor K-F, Lund-Sørensen N, Sandvik L. Serum levels of cytokines, glucose, and hemoglobin as possible predictors of poststroke depression, and association with poststroke fatigue. *Int J Neurosci*. 2012;122(11):682-690.

15. Becker K, Kohen R, Lee R, et al. Poststroke fatigue: hints to a biological mechanism. *J Stroke Cerebrovasc Dis Off J Natl Stroke Assoc.* 2015;24(3):618-621.
16. Wu S, Mead G, Macleod M, Chalder T. Model of understanding fatigue after stroke. *Stroke J Cereb Circ.* 2015;46(3):893-898.
17. Kuppuswamy A, Clark EV, Turner IF, Rothwell JC, Ward NS. Post-stroke fatigue: a deficit in corticomotor excitability? *Brain J Neurol.* 2015;138(Pt 1):136-148.
18. De Doncker W, Charles L, Ondobaka S, Kuppuswamy A. Exploring the relationship between effort perception and post-stroke fatigue. *Neurology.* Published online October 16, 2020.
19. Radman N, Staub F, Aboulafia-Brakha T, Berney A, Bogousslavsky J, Annoni J-M. Poststroke fatigue following minor infarcts: a prospective study. *Neurology.* 2012;79(14):1422-1427.
20. Russo M, Crupi D, Naro A, et al. Fatigue in patients with multiple sclerosis: from movement preparation to motor execution. *J Neurol Sci.* 2015;351(1-2):52-57.
21. Cogliati Dezza I, Zito G, Tomasevic L, et al. Functional and structural balances of homologous sensorimotor regions in multiple sclerosis fatigue. *J Neurol.* Published online December 19, 2014.
22. Sáez-Francàs N, Hernández-Vara J, Corominas-Roso M, Alegre J, Jacas C, Casas M. Relationship between poor decision-making process and fatigue perception in Parkinson's disease patients. *J Neurol Sci.* 2014;337(1-2):167-172.
23. Skapinakis P, Lewis G, Mavreas V. Temporal relations between unexplained fatigue and depression: longitudinal data from an international study in primary care. *Psychosom Med.* 2004;66(3):330-335.
24. Kuppuswamy A. The fatigue conundrum. *Brain.* 2017;140(8):2240-2245.
25. Heilman KM, Van Den Abell T. Right hemisphere dominance for attention The mechanism underlying hemispheric asymmetries of inattention (neglect). *Neurology.* 1980;30(3):327-327.
26. Kinsbourne M. Mechanisms of Unilateral Neglect. In: Jeannerod M, ed. *Advances in Psychology.* Vol 45. Neurophysiological and Neuropsychological Aspects of Spatial Neglect. North-Holland; 1987:69-86.
27. Corbetta M, Shulman GL. Control of goal-directed and stimulus-driven attention in the brain. *Nat Rev Neurosci.* 2002;3(3):201.
28. Deco G, Corbetta M. The dynamical balance of the brain at rest. *The Neuroscientist.* 2011;17(1):107-123.
29. Ferbert A, Priori A, Rothwell JC, Day BL, Colebatch JG, Marsden CD. Interhemispheric inhibition of the human motor cortex. *J Physiol.* 1992;453(1):525-546.

30. Kujirai T, Caramia MD, Rothwell JC, et al. Corticocortical inhibition in human motor cortex. *J Physiol*. 1993;471:501-519.
31. Hilgetag CC, Théoret H, Pascual-Leone A. Enhanced visual spatial attention ipsilateral to rTMS-induced 'virtual lesions' of human parietal cortex. *Nat Neurosci*. 2001;4(9):953.
32. Plewnia C, Lotze M, Gerloff C. Disinhibition of the contralateral motor cortex by low-frequency rTMS. *Neuroreport*. 2003;14(4):609-612.
33. Schambra HM, Sawaki L, Cohen LG. Modulation of excitability of human motor cortex (M1) by 1 Hz transcranial magnetic stimulation of the contralateral M1. *Clin Neurophysiol*. 2003;114(1):130-133.
34. Mevorach C, Humphreys GW, Shalev L. Opposite biases in salience-based selection for the left and right posterior parietal cortex. *Nat Neurosci*. 2006;9(6):740.
35. Netz J, Ziemann U, Hömberg V. Hemispheric asymmetry of transcallosal inhibition in man. *Exp Brain Res*. 1995;104(3):527-533.
36. Ziemann U, Hallett M. Hemispheric asymmetry of ipsilateral motor cortex activation during unimanual motor tasks: further evidence for motor dominance. *Clin Neurophysiol*. 2001;112(1):107-113.
37. Giovannelli F, Borgheresi A, Balestrieri F, et al. Modulation of interhemispheric inhibition by volitional motor activity: an ipsilateral silent period study. *J Physiol*. 2009;587(22):5393-5410.
38. Friston KJ, Kahan J, Biswal B, Razi A. A DCM for resting state fMRI. *Neuroimage*. 2014;94:396-407.
39. Irlbacher K, Brocke J, Mechow JV, Brandt SA. Effects of GABAA and GABAB agonists on interhemispheric inhibition in man. *Clin Neurophysiol*. 2007;118(2):308-316.
40. Razi A, Kahan J, Rees G, Friston KJ. Construct validation of a DCM for resting state fMRI. *Neuroimage*. 2015;106:1-14.
41. Biswal B, Zerrin Yetkin F, Haughton VM, Hyde JS. Functional connectivity in the motor cortex of resting human brain using echo-planar MRI. *Magn Reson Med*. 1995;34(4):537-541.
42. Fox MD, Raichle ME. Spontaneous fluctuations in brain activity observed with functional magnetic resonance imaging. *Nat Rev Neurosci*. 2007;8(9):700-711.
43. Flor-Henry P. Observations, reflections and speculations on the cerebral determinants of mood and on the bilaterally asymmetrical distributions of the major neurotransmitter systems. *Acta Neurol Scand*. 1986;74(S109):75-90.
44. Meyer B-U, Rörich S, Von Einsiedel HG, Kruggel F, Weindl A. Inhibitory and excitatory interhemispheric transfers between motor cortical areas in normal humans and patients with abnormalities of the corpus callosum. *Brain*. 1995;118(2):429-440.

45. Gruzelier JH. Functional neuropsychophysiological asymmetry in schizophrenia: a review and reorientation. *Schizophr Bull.* 1999;25(1):91-120.
46. Rossini PM, Tecchio F, Pizzella V, Lupoi D, Cassetta E, Paqualetti P. Interhemispheric differences of sensory hand areas after monohemispheric stroke: MEG/MRI integrative study. *Neuroimage.* 2001;14(2):474-485.
47. Toga AW, Thompson PM. Mapping brain asymmetry. *Nat Rev Neurosci.* 2003;4(1):37.
48. Lefaucheur JP, Lucas B, Andraud F, et al. Inter-hemispheric asymmetry of motor corticospinal excitability in major depression studied by transcranial magnetic stimulation. *J Psychiatr Res.* 2008;42(5):389-398.
49. Liu H, Stufflebeam SM, Sepulcre J, Hedden T, Buckner RL. Evidence from intrinsic activity that asymmetry of the human brain is controlled by multiple factors. *Proc Natl Acad Sci.* Published online 2009:pnas-0908073106.
50. Carter AR, Astafiev SV, Lang CE, et al. Resting interhemispheric functional magnetic resonance imaging connectivity predicts performance after stroke. *Ann Neurol.* 2010;67(3):365-375.
51. Di Pino G, Pellegrino G, Assenza G, et al. Modulation of brain plasticity in stroke: a novel model for neurorehabilitation. *Nat Rev Neurol.* 2014;10(10):597-608.
52. Blumberger DM, Vila-Rodriguez F, Thorpe KE, et al. Effectiveness of theta burst versus high-frequency repetitive transcranial magnetic stimulation in patients with depression (THREE-D): a randomised non-inferiority trial. *The Lancet.* 2018;391(10131):1683-1692.
53. Friston K, Mattout J, Trujillo-Barreto N, Ashburner J, Penny W. Variational free energy and the Laplace approximation. *Neuroimage.* 2007;34(1):220-234.
54. Friston K, Zeidman P, Litvak V. Empirical Bayes for DCM: a group inversion scheme. *Front Syst Neurosci.* 2015;9:164.
55. Craig AD. Forebrain emotional asymmetry: a neuroanatomical basis? *Trends Cogn Sci.* 2005;9(12):566-571.

Figure legends

Figure 1. Neural connectivity computational model architecture. This figure represents the dynamic causal model architecture consisting of 11 brain regions selected from NeuroSynth tool (<http://neurosynth.org/>; ventromedial prefrontal cortex (vmPFC), left and right anterior insula, supplementary motor area (SMA), left and right caudate head, left and right primary motor cortex (M1), left and right thalamus and posterior cingulate cortex (PCC)). The model was fully connected, consisting of 110 extrinsic (between regions) influences, and 11 intrinsic (within region) influences. Depicted are the 8 inter-hemispheric influences, other connections are left out from the figure for clarity. We used this biologically plausible dynamic causal model to find the best fit or explain the recorded fluctuations in BOLD intensities.

Figure 2. rs-fMRI inter-hemispheric inhibition balance in M1 and fatigue severity.

Figure shows a relationship between IIB indices [L to R minus R to L influence] and self-reported fatigue severity scores in Experiment 1. The inter-hemispheric inhibition balance (IIB) was computed by subtracting R to L M1 effect sizes from L to R M1 effect sizes. Negative IIB values on the x-axis reflect overall stronger inhibitory L to R influence, whereas positive values reflect overall stronger inhibitory R to L influence. Strength of effective connectivity inferred from sp-DCM is represented by a percentage change in activity (effect size) in an area (e.g. right M1), as a consequence of activity change in another area (i.e. left M1). Grey circles mark participants with the left-hemisphere lesion, black circles mark participants with the right-hemisphere lesion.

Figure 3. pp-TMS inter-hemispheric inhibition balance in M1 and fatigue severity.

Figure shows a relationship between IIB indices in M1 [L to R minus R to L effect] and self-reported fatigue severity scores in Experiment 2. The inter-hemispheric inhibition balance (IIB) was computed by subtracting R to L M1 effect sizes from L to R M1 effect sizes. Negative IIB values on the x-axis reflect overall stronger inhibitory L to R effect, whereas positive values reflect overall stronger inhibitory R to L effect. Strength of effective connectivity measured with pp-TMS is represented by a percentage change in activity (effect size) in an area (e.g. right M1), as a consequence of activity change in another area (i.e. left M1). Grey circles mark participants with the left-hemisphere lesion, black circles mark participants with the right-hemisphere lesion.

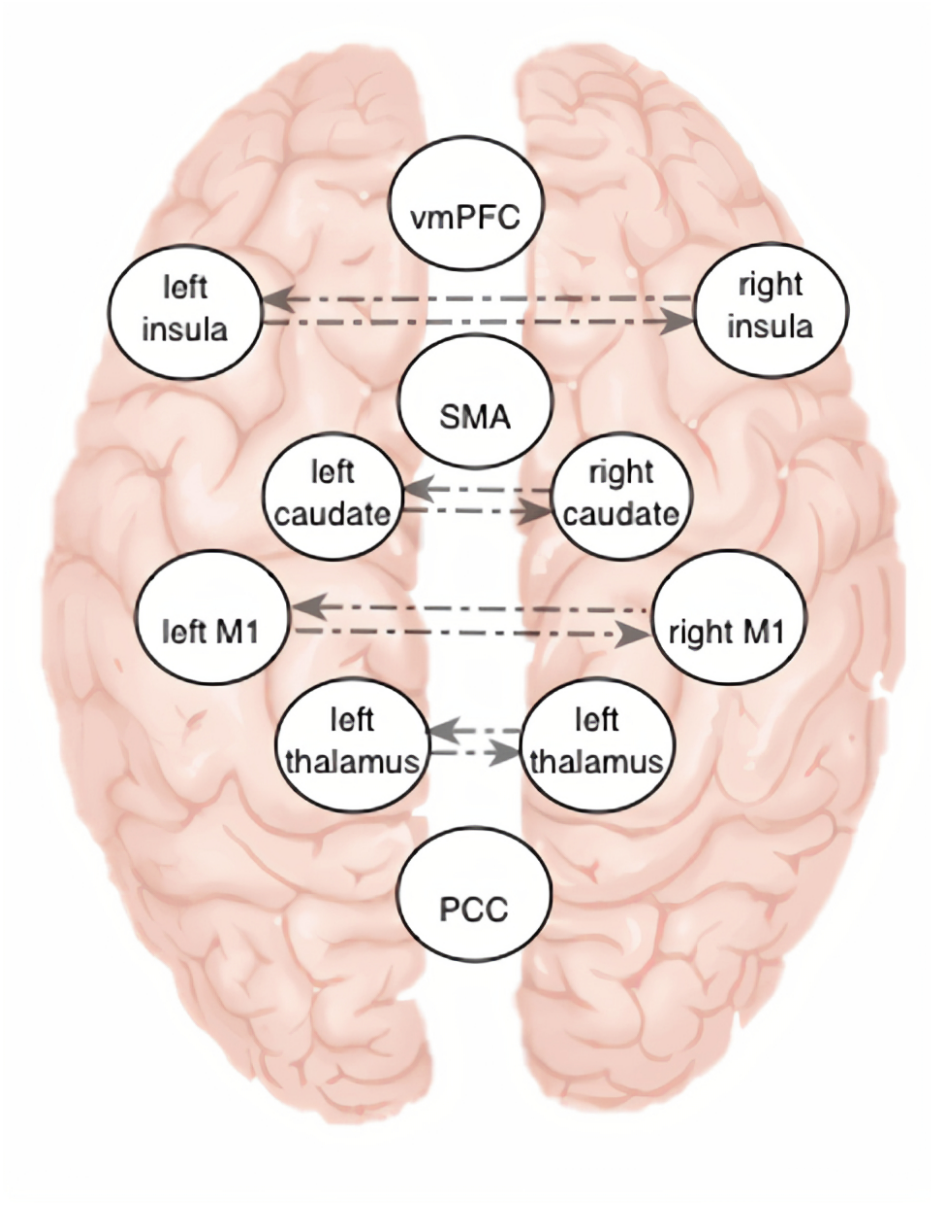


Figure 1

881x1121mm (28 x 28 DPI)

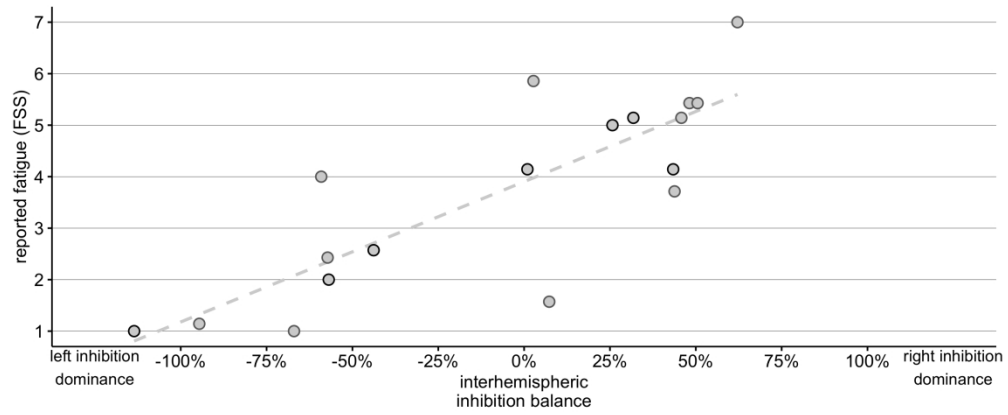


Figure 2

72390x30480mm (1 x 1 DPI)

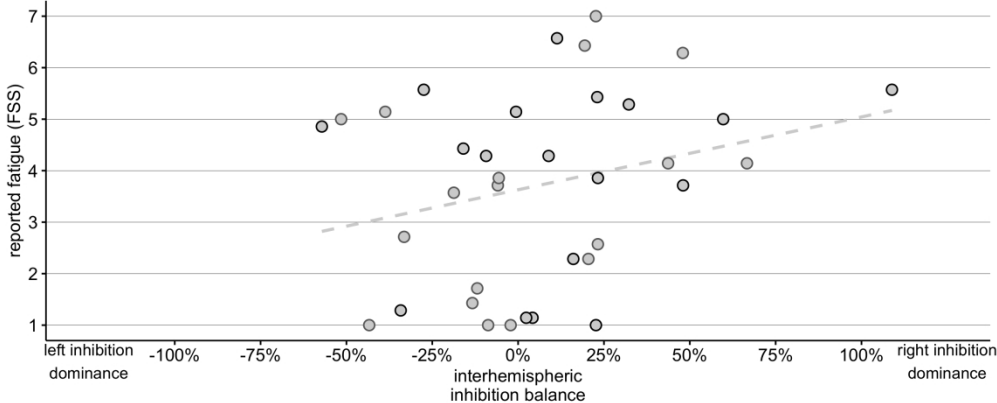


Figure 3

72390x30480mm (1 x 1 DPI)

Table 1 Effective connectivity summary

| | Effect size (Hz) LtoR M1 | Effect size (Hz) RtoL M1 | IHI index |
|------|--------------------------|--------------------------|-----------|
| Pp1 | 0.274 | -0.347 | 0.621 |
| Pp2 | 0.935 | 0.430 | 0.505 |
| Pp3 | -0.242 | 0.196 | -0.438 |
| Pp4 | -0.616 | -0.047 | -0.569 |
| Pp5 | -0.589 | 0.547 | -1.136 |
| Pp6 | 0.006 | -0.021 | 0.027 |
| Pp7 | 0.154 | -0.165 | 0.319 |
| Pp8 | 0.134 | 0.061 | 0.073 |
| Pp9 | 0.303 | 0.046 | 0.257 |
| Pp10 | 0.137 | 0.127 | 0.010 |
| Pp11 | -0.058 | -0.540 | 0.482 |
| Pp12 | -0.350 | 0.241 | -0.591 |
| Pp13 | 0.343 | 1.289 | -0.946 |
| Pp14 | -0.329 | 0.341 | -0.670 |
| Pp15 | 0.131 | -0.327 | 0.458 |
| Pp16 | 0.189 | -0.249 | 0.438 |
| Pp17 | 0.148 | -0.286 | 0.434 |
| Pp18 | -0.335 | 0.237 | -0.572 |

Table shows a summary of the estimated M1 interhemispheric effective connectivity effect sizes and the computed IHI from Experiment 1. [Pp = participant].

Table 2 Stroke summary

| | Hemisphere | Location | Stroke type |
|------|------------|-------------------|--------------|
| Pp1 | Left | Parietal cortex | Ischaemic |
| Pp2 | Left | Putamen | Ischaemic |
| Pp3 | Right | Parietal cortex | Ischaemic |
| Pp4 | Left | Prefrontal cortex | Ischaemic |
| Pp5 | Right | External capsule | Ischaemic |
| Pp6 | Left | Temporal cortex | Ischaemic |
| Pp7 | Right | Corona radiata | Ischaemic |
| Pp8 | Left | Prefrontal cortex | Ischaemic |
| Pp9 | Right | Internal capsule | Ischaemic |
| Pp10 | Right | Parietal cortex | Ischaemic |
| Pp11 | Left | Parietal cortex | Haemorrhagic |
| Pp12 | Left | Parietal cortex | Haemorrhagic |
| Pp13 | Left | Putamen | Ischaemic |
| Pp14 | Left | External capsule | Ischaemic |
| Pp15 | Left | Pons | Ischaemic |
| Pp16 | Left | Fronto-parietal | Haemorrhagic |
| Pp17 | Right | Putamen | Ischaemic |
| Pp18 | Left | Insula | Ischaemic |

Table shows a summary of the stroke-affected hemisphere, locations and type of the stroke from Experiment 1. [Pp = participant].

Table 3 Participants' demographics

| | Experiment 1 (N = 18) | Experiment 2 (N = 41) | <i>p</i> -value |
|---------------------------------|--------------------------|--------------------------|-------------------|
| Gender, females:males | 2:16 | 9:32 | <i>p</i> = 0.4756 |
| Hemisphere affected, left:right | 12:6 | 20:21 | <i>p</i> = 0.4122 |
| Age, years | 58.68 (10.30) | 62.37 (12.63) | <i>p</i> = 0.1691 |
| Time Since Stroke, years | 4.03 (3.97) | 5.46 (5.76) | <i>p</i> = 0.2416 |
| Grip, % unaffected hand | 88.67 (22.14) | 95.55 (15.45) | <i>p</i> = 0.3471 |
| NHPT, % unaffected hand | 77.73 (33.06) | 89.31 (22.38) | <i>p</i> = 0.3066 |
| SDMT | 1.25 (0.42) | 1.18 (0.46) | <i>p</i> = 0.6187 |
| Fatigue – FSS | 3.71 (1.87) | 3.65 (1.98) | <i>p</i> = 0.8302 |
| Depression – HADS | 4.28 (3.27) | 4.59 (3.33) | <i>p</i> = 0.6020 |
| Anxiety – HADS | 6.50 (5.45) | 5.22 (3.91) | <i>p</i> = 0.6083 |

Values are presented as mean (SD).

Table presents an overview of participants' demographics, and several measure of their physical and mental states separately for experiments 1 and 2. Last column shows *p*-values for the comparison between the experiments.